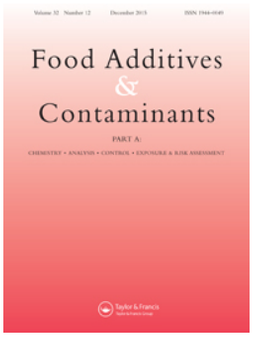

Food Additives & Contaminants: Part A

ISSN: 1944-0049 (Print) 1944-0057 (Online) Journal homepage: http://www.tandfonline.com/loi/tfac20

Estimation of residue depletion of cyadox and its marker residue in edible tissues of pigs using physiologically based pharmacokinetic modelling

Lingli Huang, Zhoumeng Lin, Xuan Zhou, Meiling Zhu, Ronette Gehring, Jim E. Riviere & Zonghui Yuan

To cite this article: Lingli Huang, Zhoumeng Lin, Xuan Zhou, Meiling Zhu, Ronette Gehring, Jim E. Riviere & Zonghui Yuan (2015) Estimation of residue depletion of cyadox and its marker residue in edible tissues of pigs using physiologically based pharmacokinetic modelling, Food Additives & Contaminants: Part A, 32:12, 2002-2017, DOI: 10.1080/19440049.2015.1100330

To link to this article: http://dx.doi.org/10.1080/19440049.2015.1100330

Food Additives & Contaminants: Part A, 2015
Vol. 32, No. 12, 2002–2017, http://dx.doi.org/10.1080/19440049.2015.1100330

Taylor & Francis
Taylor & Francis Group

Estimation of residue depletion of cyadox and its marker residue in edible tissues of pigs using physiologically based pharmacokinetic modelling

Lingli Huang[a,b,c], Zhoumeng Lin[d], Xuan Zhou[d], Meiling Zhu[d], Ronette Gehring[b], Jim E. Riviere[b]* and Zonghui Yuan[a,c,d]*

[a]*MOA Laboratory of Risk Assessment for Quality and Safety of Livestock and Poultry Products, Huazhong Agricultural University, Wuhan, 430070, China;* [b]*Institute of Computational Comparative Medicine (ICCM), College of Veterinary Medicine, Kansas State University, Manhattan, KS 66506, USA;* [c]*Hubei Collaborative Innovation Center for Animal Nutrition and Feed Safety, Huazhong Agricultural University, Wuhan, 430070, China;* [d]*National Reference Laboratory of Veterinary Drug Residues (HZAU) and MAO Key Laboratory for Detection of Veterinary Drug Residues, Huazhong Agricultural University, Wuhan, 430070, China*

(*Received 2 June 2015; accepted 22 September 2015*)

Physiologically based pharmacokinetic (PBPK) models are powerful tools to predict tissue distribution and depletion of veterinary drugs in food animals. However, most models only simulate the pharmacokinetics of the parent drug without considering their metabolites. In this study, a PBPK model was developed to simultaneously describe the depletion in pigs of the food animal antimicrobial agent cyadox (CYA), and its marker residue 1,4-bisdesoxycyadox (BDCYA). The CYA and BDCYA sub-models included blood, liver, kidney, gastrointestinal tract, muscle, fat and other organ compartments. Extent of plasma-protein binding, renal clearance and tissue-plasma partition coefficients of BDCYA were measured experimentally. The model was calibrated with the reported pharmacokinetic and residue depletion data from pigs dosed by oral gavage with CYA for five consecutive days, and then extrapolated to exposure in feed for two months. The model was validated with 14 consecutive day feed administration data. This PBPK model accurately simulated CYA and BDCYA in four edible tissues at 24–120 h after both oral exposure and 2-month feed administration. There was only slight overestimation of CYA in muscle and BDCYA in kidney at earlier time points (6–12 h) when dosed in feed. Monte Carlo analysis revealed excellent agreement between the estimated concentration distributions and observed data. The present model could be used for tissue residue monitoring of CYA and BDCYA in food animals, and provides a foundation for developing PBPK models to predict residue depletion of both parent drugs and their metabolites in food animals.

Keywords: cyadox; 1,4-bisdesoxycyadox; PBPK modelling; tissue depletion; residue prediction; sensitivity analysis; Monte Carlo analysis

Introduction

Violative residues of veterinary drugs in animal-derived foods are a great challenge to global food safety (Baynes and Riviere 2014). Traditional surveillance of veterinary drug residues relies on their detection in incurred samples, which is expensive and time-consuming. Over the past few decades, several methods have been developed to predict the residue profile of veterinary drugs in food animals, including traditional pharmacokinetic (Mercer et al. 1977; Riviere 2011) as well as tissue-body fluid (blood and urine) correlation approaches (Chiesa, von Bredow, Nochetto et al. 2006; Chiesa, von Bredow, Smith et al. 2006; Liu et al. 2010; Yang et al. 2010). However, these methods cannot describe continuous tissue residue profiles under various exposure scenarios. Their lack of physiological roots also prevents these empirical approaches from quantitating effects of specific physiological or disease states on drug disposition and residue depletion.

Physiologically based pharmacokinetic (PBPK) modelling is a computational technique that incorporates species-specific physiological parameters and chemical-specific dynamic information to simulate the absorption, distribution, metabolism, and excretion of compounds in the body. A PBPK model is an excellent tool for the prediction of veterinary drug residues because it can be used to simulate continuous tissue residue time–concentration profiles and allows extrapolation across exposure routes, doses, and species. Several PBPK models have been developed to predict veterinary drug residues in food animals (Craigmill 2003; Buur et al. 2006, 2008; Cortright et al. 2009; Leavens et al. 2012, 2014). All of these models successfully simulated the depletion of parent drug, with only two recent models describing the kinetics of their metabolites (Yang, Huang, et al. 2014; Yang et al. 2015). To date, no single model has linked the disposition of both moieties which is crucial since food safety is estimated from total drug and metabolite

*Corresponding authors. Email: jriviere@ksu.edu (Jim E. Riviere); yuan5802@mail.hzau.edu.cn (Zonghui Yuan)

exposure, but is then monitored based only on either the parent drug or one metabolite serving as a marker residue. A comprehensive model describing both is important for a realistic risk profile to be established.

Cyadox (CYA) is a synthetic 1,4-dioxide quinoxaline antimicrobial agent for use in food-producing animals, including pigs and chicken (Wang et al. 2005; Ding, Wang et al. 2006, Ding, Yuan et al. 2006). CYA is less toxic than its congeners, olaquindox and carbadox (He et al. 2006; Huang et al. 2010; Wang, Fang, et al. 2011; Wang, He, et al. 2011). However, excessive exposure to CYA has been reported to cause adverse effect on mouse and human microflora (Hao et al. 2013; Huang et al. 2013).

A recent study reported CYA pharmacokinetics after oral administration (Zhao et al. 2013). Once absorbed, CYA is extensively metabolised in the liver and intestine, producing a number of metabolites, with BDCYA (1,4-bisdesoxycyadox) being the main metabolite and designated as the marker residue in some jurisdictions (Liu et al. 2009; Wu et al. 2012; Huang et al. 2015). BDCYA, the N-oxide reduction product of CYA, is formed by reducing oxygen on both the N1 and N4 sites on the benzene moiety which would lead to DNA damage by intermediate radical production (Badham & Winn 2010; Huang et al. 2010). Hence, BDCYA could be a potential toxic metabolite of CYA, and should be considered together with the parent drug for food safety concerns. Pharmacokinetic and residue depletion of CYA in pigs after oral and dietary exposures have been reported (Li et al. 2013; Qiu 2012; Zhao et al. 2013) with CYA and BDCYA depletion being relatively rapid in tissues of pigs. A PBPK model for quinoxaline-2-carboxylic acid (QCA), one of the CYA metabolites, was developed in rats and pigs (Yang et al. 2015).

Based on the extensive data available for CYA and BDCYA in pigs, the objective of the present study was to develop a PBPK model to simultaneously simulate the concentrations of CYA and BDCYA in liver, kidney, muscle and fat after oral gavage dosage and feed administration to pigs. To aid model development, several additional experiments were conducted to obtain key model parameters, including plasma-protein binding, renal clearance and tissue-plasma partition coefficients of BDCYA. Finally, an additional pharmacokinetic study of CYA in pigs after 14-day feed exposure was conducted to further evaluate model performance.

Materials and methods

Experimental studies for model development

Chemicals and reagents

The premix of CYA (5%) was provided by the Institute of Veterinary Pharmaceuticals (Wuhan, China). Standards of CYA (>99.0%) and BDCYA (98.5%) were obtained from the Institute of Veterinary Pharmaceuticals (Huazhong Agricultural University, Wuhan, China). Stock solutions (1.0 mg/mL) were prepared by dissolving CYA and BDCYA in dimethylsulfoxide. Working mixed standard solutions (0.01 mg/mL) were prepared by diluting the stock solution with methanol. All solutions were kept in brown containers and stored at −20°C.

Animals

Thirty-three healthy castrated crossbred (Duroc × Large white × Landrace) pigs (80 days old, weight 15–35 kg) were purchased from the Livestock and Poultry Breeding Centre of Hubei Province (Wuhan, China). The pigs were fed with a basal diet without antimicrobial agents/compounds and acclimatised for one week before the experiment. Pigs were housed in six 8 m × 10 m pens under standard environmental conditions (25 ± 2°C; 45–65% relative humidity). Feed was withheld approximately 12 h before until 4 h after drug administration, while water was available *ad libitum*. The experimental procedures involving animals in this study were approved by the Animal Care Centre, Hubei Academy of Medical Sciences.

Experiment 1: plasma protein binding of CYA and BDCYA

The plasma protein bindings of CYA and BDCYA were determined using the equilibrium dialysis method (Cheng et al. 2013). Fresh blank pig plasma samples (n = 15, 1 mL each) were placed into 15 dialysis bags (molecular-weight cut-off 8000–14,000 Da) and incubated with 10 mL of different concentrations (0.05, 0.5 and 1.0 μg/mL) of CYA and BDCYA in phosphate buffer at 4°C for 48 h. One hundred micro-litre dialysis filtrate solutions were sampled and analysed by HPLC as described below. The value of plasma protein binding was equal to the amount of bound drug divided by the total amount added:

$$\mathrm{Pb} = \frac{D_t - D_f}{D_t} \times 100\% \quad (1)$$

where Pb is the plasma protein binding percentage, D_t is the amount in blood, and D_f is the amount in phosphate buffer.

Experiment 2: renal clearance of CYA and BDCYA

Pigs (20 ± 5.8 kg, n = 4) were injected with 1.5 mg/kg of CYA through the ear vein, and then with 1.5 mg/kg of BDCYA after a washout period of 10 days. Blood samples (5 mL) were collected via precava before and 3 h after administration. Urine samples were collected and volumes recorded every 6 h. Plasma samples (0.4 mL) were decanted into a clean centrifuge tube (1.5 mL, vortex-mixed with 4 mL methanol for 2 min), and centrifuged (10,000 r/min, 25°C, 10 min).

The supernatants were filtered with 0.22 μm filtration membrane and the filtered solutions analysed by HPLC. Urine samples (2 mL) were mixed with water (4 mL) and processed with HLB column. The Oasis HLB cartridge (3 mL, 60 mg, Waters column) was conditioned by passing 3 mL methanol followed by 3 mL water, and then the prepared urine samples were loaded onto the cartridge, washed with 3 mL water/methanol (90/10, v/v), followed by one additional washing with 3 mL methanol. Eluates were extracted two times with methylene dichloride, taken to dryness under a stream of nitrogen at 45°C. The residue was dissolved with methanol (1 mL) followed by vortexing for 1 min. The solutions were then passed through the filtration membrane (0.22 um) for HPLC analyses.

The HPLC consisted of a Waters 2695 pump and 2487 UV detector. An Eclipse XDB-C18 HPLC column (250 mm × 4.6 μm) was used for sample separation. The mobile phase consisted of acetonitrile/water (18/82 v/v for CYA, 22/78 v/v for BDCYA). The flow rate was 1.0 mL/min. The wavelength was programmed at 320 nm for CYA and then switched to 280 nm for BDCYA. The value of renal clearance was calculated as the rate of excretion of CYA and BDCYA in urine divided by the plasma concentration at the midpoint time of urine collection:

$$\mathrm{Cl} = \frac{dX/dt}{C_b} \tag{2}$$

where Cl is the renal clearance, C_b is the concentration of the compound in plasma at the midpoint time of urine collection, X is the amount of the compound in urine and t is the time of urine collection (Riviere 2011).

Experiment 3: tissue/plasma partition coefficient

BDCYA solution (0.5 mg/mL) was infused into pigs (20 ± 4.0 kg, n = 4) via the ear vein at a rate of 2 mL/min for 60 min (3.0 mg/kg b.w.) until the concentration of BDCYA in plasma reached the steady state. Subsequently, all pigs were slaughtered using captive bolt stunning equipment and exsanguinated on the basis of guidelines provided by the American Veterinary Medical Association for euthanasia (AVMA 2001). Blood, liver, kidney, fat, and muscle samples were collected and analysed using a HPLC method previously described (Zhang et al. 2005) with minor modifications. Briefly, homogenates of each tissue sample (2.00 g) were mixed with ethyl acetate solution (4 mL) in a polyethylene tube (20 mL), followed by 2 min vortexing and 10 min centrifugation (3500 r/min, 25°C). The supernatant was decanted, and the residues were twice extracted by ethyl acetate. The extractions were combined and dried under a stream of nitrogen at 50°C, followed by addition of methyl cyanides (2 mL) and then 1 min vortexing. N-hexane (3 mL) was added to remove fat and twice repeated. Finally, this was extracted with acetonitrile, dried under a stream of nitrogen at 50°C, and then 1 mL methanol added and vortex-mixed for 1 min. All solutions were then analysed with HPLC using the same method as for the plasma and urine samples described above. The partition coefficients for non-eliminating tissues (liver, muscle and fat) and eliminating tissue (kidney) were calculated using Equations (3) and (4), respectively, as follows:

$$P_t = \frac{C_{t,SS}}{C_{b,SS}} \tag{3}$$

$$P_t = \frac{C_{t,SS}}{C_{b,SS}\cdot(1-E)} \tag{4}$$

where P_t represented the tissue-to-plasma partition coefficients of BDCYA; $C_{t,ss}$ and $C_{b,ss}$ are the steady-state concentrations of BDCYA in tissues (muscle, liver, adipose and kidney) and plasma, respectively; and E is the renal extraction ratio calculated as renal clearance divided by the blood flow to kidney.

Experiment 4: residue depletion study of cyadox in pigs

Twenty-five healthy pigs, weighing 30 ± 2.5 kg (80 days old), were divided into five groups, and fed with medicated feed at 200 mg/kg for consecutive 14 days. At 0.25, 1, 3, 7 and 14 days after the end of exposure, pigs (n = 5/time point) were slaughtered as described above in Experiment 3. Liver, kidney, muscle and fat samples were collected and stored at −20°C until analysis. Each tissue sample (2.0 ± 0.01 g) was mixed with 1% metaphosphoric acid (6 mL) in methanol/acetonitrile/water (50:10:40, v/v/v) in a 50 mL polypropylene centrifuge tube, followed by centrifugation for 10 min at 4000g. The supernatants were then mixed with 1% metaphosphoric acid, and extraction solutions loaded onto the HLB column (60 mg, 3 mL) previously pre-conditioned with methanol (3 mL) and water (3 mL). The column was washed with water (3 mL) and 10% methanol (3 mL), and then eluted with methanol at a flow rate of 1.0 mL/min into a 10 mL polypropylene tube and diluted by 2% metaphosphoric acid (3 mL). All flow rates for conditioning and washing were lower than 3 mL/min. Next, chloroform (6 mL × 2) was added to the extracted solutions and the contents were mixed for 2 min and centrifuged for 10 min at 4000g. The lower layer was transferred into a 50 mL centrifuge tube, 200 μL 10% sodium hydroxide solution added and the third back extraction was repeated. The three back extracts were then combined and evaporated to dryness under a stream of nitrogen at 40°C. The residue was dissolved with 400 μL acetonitrile/water (15:85, v/v). The solution was then filtered through a 0.22 μm nylon Millipore chromatographic filter for HPLC analysis. The HPLC analysis procedure was the same

as described in experiment 3 except that the mobile phase was changed to the following gradient profile (t in min): $t_{0'}$, A = 15%, B = 85%; $t_{4'}$, A = 30%, B = 70%; $t_{25'}$, A = 15%, B = 85%.

The method was validated with reference to the validation procedure for residues in food animal products as described in the EU Commission Decision 2002/657/EC under Council Directive 96/23/EC. The validation metrics of specificity, linearity, limit of detection and quantitation (LOD and LOQ), accuracy and precision for the method were determined. The blank tissue samples were spiked with CYA and BDCYA at each of three concentrations (20, 40 and 80 µg/kg) to estimate the recovery and standard deviation. Figure 1 shows this method had excellent specificity because no interference was observed in the retention time of CYA and BDCYA. The validation results showed that the LOQ for CYA and BDCYA was 0.02 mg/kg and the linearity of CYA and BDCYA was Y = 65.816× – 2093.2 (r = 0.999) and Y = 88.986× – 500.4 (r = 0.998), respectively. The recoveries of CYA and BDCYA in different tissues ranged from 68.8% to 87.5% with a intraday relative standard deviation of less than 11%.

PBPK model development

Data source for model calibration. The data used to calibrate the model for CYA and BDCYA are from Li et al. (2013). Briefly, 35 healthy adult pigs were randomly divided into seven groups and treated with CYA by oral gavage at a dosage of 20 mg/kg for 5 days. Pigs (n = 5) were randomly slaughtered at 12, 24, 72, 120, 168, 216, and 264 h after the last dosing, and tissue samples (muscle, liver, kidney, and fat) were collected and analysed for the concentrations of CYA and its metabolites including BDCYA via a liquid chromatography-tandem mass spectrometry method (Li et al. 2013).

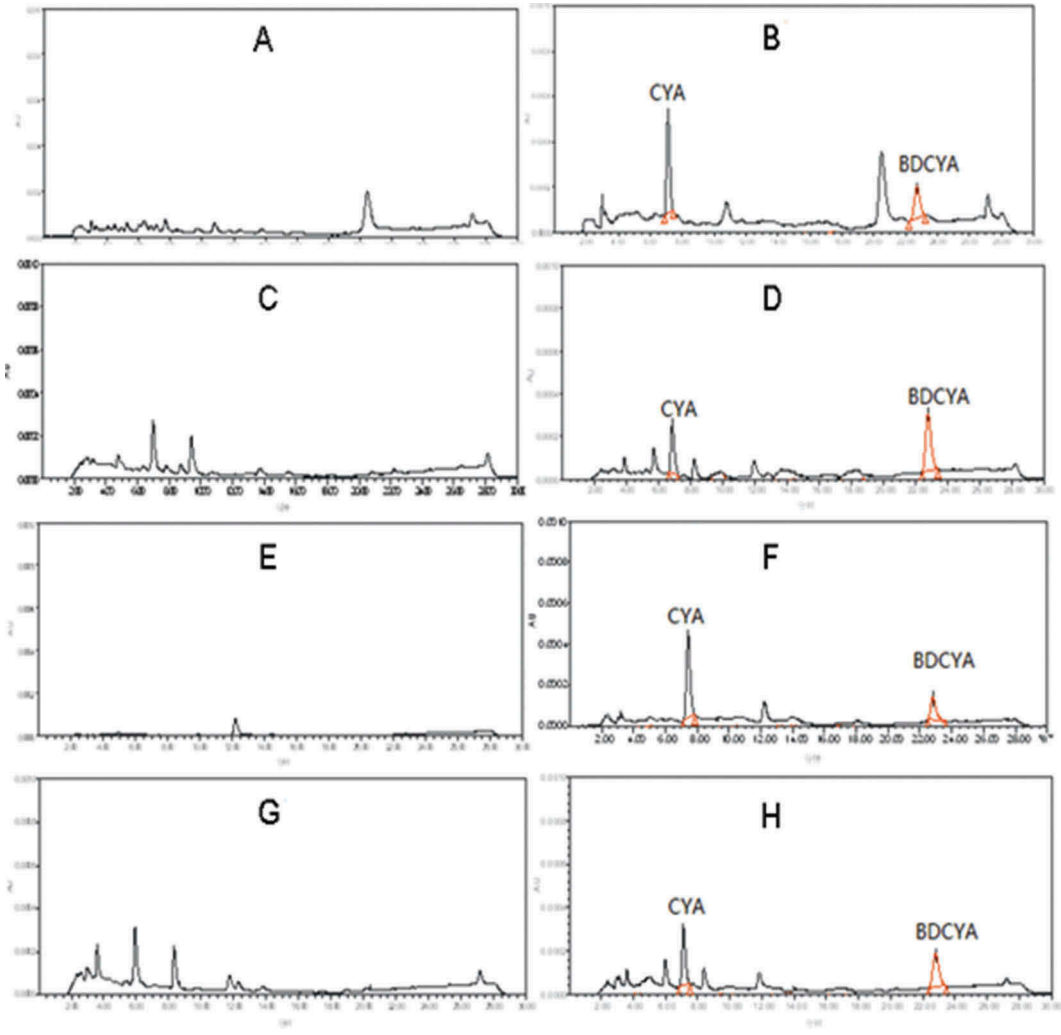

Figure 1. Chromatograms of the pig liver, kidney, muscle and fat spiked with standards of CYA and BDCYA at 20 µg/kg.
Note: A, C, E, G: blank liver, kidney, muscle and fat, respectively; B, D, F, H: spiked liver, kidney, muscle and fat, respectively.

Software for PBPK model development

AcslX simulation software (Version 3.0.2.1, AEgis Technologies Group, Inc., Huntsville, AL, USA) was used for all modelling work including parameter estimation, local sensitivity analysis, and model predictions with the point estimates and upper and lower uncertainty limits. Model code is available from our website (http://iccm.k-state.edu/).

Model structure

The model was composed of two sub-models for CYA and its main metabolite BDCYA, with each sub-model consisting of seven compartments (blood, liver, kidney, adipose, muscle, gastrointestinal tract, and others; Figure 2). Liver, kidney, adipose, and muscle compartments were included because these organs are common edible tissues and relevant to food safety. Blood was included as it is the essential compartment connecting all other compartments via systemic circulation. Since CYA was dosed to animals by oral or feed administration, the gastrointestinal tract was assumed the primary absorption site and modelled as an independent compartment. Additionally, a lumped compartment representing the other organs is necessary in order to account for disposition of the drug and its metabolite to the rest of the body. Faecal and urinary pathways were the major excretion routes of CYA and its metabolites (Huang et al. 2015). Radiotracer studies have demonstrated that more than 50% and 44% of the total drug could be excreted from the faeces and urine, respectively (Huang et al. 2015), and several metabolites could be detected in liver and intestinal fluid when CYA was incubated with liver microsomes and intestinal microflora (Liu et al. 2009; Xu et al. 2011). Hence, kidney, liver and gastrointestinal tract were selected as the main compartments for metabolism and elimination. The present model was constructed based on the following assumptions. All compartments were well mixed and flow-limited. Hepatic and enteric metabolism of CYA was described using a first-order rate process. Eliminations of CYA and BDCYA occurred into urine, bile and faeces, which were also described using a first-order rate process.

Absorption

The uptake of CYA was described based on Lin et al. (2011) with some modifications. In brief, CYA is distributed into the intestinal lumen after gastric emptying described by the rate constant Kst (h^{-1}). This is followed by CYA absorption from the intestinal lumen into the GI tract's bloodstream, with an intestinal absorption rate constant Ka (h^{-1}). Based on the radiotracer study and *in vitro* metabolism of CYA, more than 50% of the dosage could be excreted in faeces (Huang et al. 2015), with CYA being further metabolised in the intestine into BDCYA (Xu et al. 2011); Kef and Km2 were used to describe the faecal

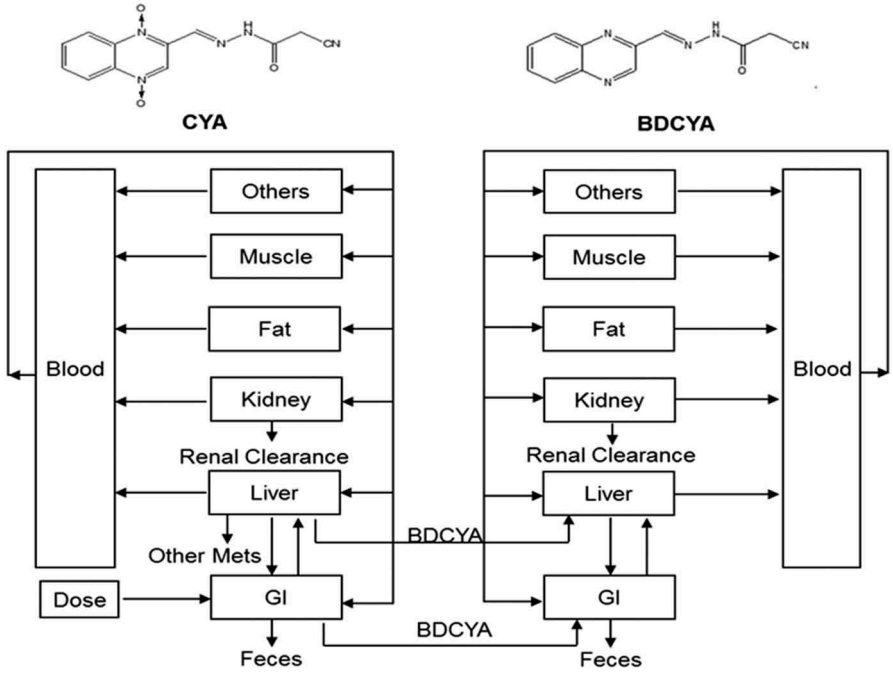

Figure 2. Physiologically based pharmacokinetic model structure for cyadox (CYA) and 1,4-bisdesoxycyadox (BDCYA) in pigs exposed to CYA by oral gavage or in feed.

excretion and intestine metabolism of CYA, respectively. Therefore, the rate of CYA decay at the intestinal absorption site was described as follows:

$$RI = Kst * AST - Ka * AI - Kef * AI - Km2 * AI \quad (5)$$

where RI is the rate of CYA loss in the intestine, μM/h; AST is the amount of CYA in the stomach, μM; AI is the amount of CYA in the intestine, μM; Kst is the gastric-emptying rate constant, h^{-1}; Ka is the absorption rate constant, h^{-1}; Kef is the intestinal transit rate constant, h^{-1}; and Km2 is the metabolism rate constant of CYA in the intestine, h^{-1}.

Distribution

The rate of change for both CYA and BDCYA in each compartment was described using mass balance differential equations (Lin et al. 2013, 2015; Leavens et al. 2014). Based on the assumption that all compartments are flow-limited, a compound's distribution is determined by a process rate-limited by blood flow. As an example, the flow-limited liver compartment differential rate equation for CYA is:

$$RL = QL*(CA - CVL) + RAO - Rmet - Rbile \quad (6)$$

where RL is the rate of distribution of CYA in the liver, μM/h; QL is the volume of blood flow to the liver per hour, l/h; CA is the arterial blood concentration of CYA, μM; CVL is the liver venous blood concentration of CYA, μM; RAO is the absorption rate of CYA from the GI tract via portal vein, μM/h; Rmet is the metabolism rate of CYA in the liver, μM/h; and Rbile is the elimination rate of CYA from the bile, μM/h.

Metabolism

The model described the metabolism of CYA to BDCYA and other metabolites in the liver using the first-order rate equations as follows:

$$Rmet = Km1 * CVL \quad (7)$$

where Km1 is the total metabolism rate constant of CYA in the liver, /h; and CVL is the liver venous blood concentration of CYA, μM.

Elimination

A separate experiment was conducted to determine urine elimination as described using the following equation based on Lin et al. (2015):

$$Rurine = Keu * CVK \quad (8)$$

$$Keu = CLcya * BW \quad (9)$$

where Rurine is the elimination rate of CYA via the urine, μM/h; Keu is the urine elimination rate constant for CYA, L/h; and CVK is the kidney venous blood concentration of CYA, μM. CLcya is the renal clearance of CYA in pigs which was obtained from Experiment 1, L/(h*kg). BW is the body weight, kg.

Based on the radiotracer study, high concentrations of radioactivity could be detected in the bile of pigs, indicating that biliary excretion is another major route of CYA elimination. Hence, the following equation was used to describe the bile excretion rate:

$$Rbile = Kb * CVL \quad (10)$$

where Rbile is the elimination rate of CYA via the bile, μM/h; Kb is the bile elimination rate constant for CYA, L/h; and CVL is the kidney venous blood concentration of CYA, μM.

Model parameterisation

Physiological parameters including organ volumes, blood flow rates and body weight for pigs, were obtained from published sources (Table 1). Most of the chemical-specific parameters were estimated by the model based on the previous studies. For example, the radiotracer study showed that more than 44% of the total drug could be observed in the urine of pigs within 7 days after a single oral administration of [^{3}H]-CYA, suggesting that the bioavailability of CYA should be at least 44%. Although biliary excretion was observed, the amount accounted for less than 1% of the total drug dosed. Based on these results, we set the bioavailability to be 0.44. Since CYA can be metabolised in the intestine, and both the parent drug and the metabolites can be absorbed in the small intestine at different rates, we estimated the absorption rate constant of the parent drug (Ka) and BDCYA (Ka1) by visually fitting to the plasma concentrations from a pharmacokinetic study where CYA was orally dosed (Zhao et al. 2013). The faecal elimination rate constants of CYA (Kef) and BDCYA (Kef1) were estimated based on the concentrations of CYA and BDCYA in faeces from Xu et al. (2012).

Table 1. Physiological parameters for the pig used in the PBPK modelling process.

Parameter	Description	Value	Sources
Blood flow rates			
QCC	Cardiac output (L/h/kg)	5.0	Upton (2008)
QLC	Fraction of blood flow to the liver	0.27	Average of Buur et al. (2005) and Upton (2008)
QKC	Fraction of blood flow to the kidney	0.12	Average of Buur et al. (2005) and Upton (2008)
QMC	Fraction of blood flow to the muscle	0.25	Average of Buur et al. (2005) and Upton (2008)
QFC	Fraction of blood flow to the fat	0.13	Average of Buur et al. (2005) and Upton (2008)
QGC	Fraction of blood flow to the intestines	0.18	Tranquilli et al. (1982)
Tissue volumes			
VbloodC	Fraction of body weight as blood	0.06	Average of Buur et al. (2005) and Upton (2008)
VLC	Fraction of body weight as liver	0.025	Average of Buur et al. (2005) and Upton (2008)
VKC	Fraction of body weight as kidney	0.004	Average of Buur et al. (2005) and Upton (2008)
VMC	Fraction of body weight as muscle	0.40	Average of Buur et al. (2005) and Upton (2008)
VFC	Fraction of body weight as fat	0.32	Average of Buur et al. (2005) and Upton (2008)
VGC	Fraction of body weight as intestines	0.05	Upton (2008)

Table 2. Plasma protein binding percentage of CYA and BDCYA in pigs.

Drug	Concentration (μg/mL)	Plasma protein binding percentage (%)			
		1	2	3	Mean ± SD
CYA	0.05	15.15	15.71	13.93	14.93 ± 0.91
	0.5	17.60	16.12	14.81	16.18 ± 1.40
	1	15.28	14.57	14.29	14.71 ± 0.51
BDCYA	0.05	71.85	70.10	70.09	70.68 ± 0.83
	0.5	73.62	72.91	70.75	72.43 ± 1.22
	1	73.21	74.10	73.49	73.60 ± 0.37

The initial value of Kst was set to be 0.25 as the literature reported (Buur et al. 2006), and adjusted according to the administration route. The renal clearance of CYA and BDCYA and the tissue/plasma partition coefficients of BDCYA were determined in Experiments 2 and 3, respectively. The initial values for partition coefficients of CYA in tissues and plasma were set to be the same as BDCYA, and subsequently further adjusted by fitting to the residue depletion data reported by Li et al. (2013).

There were two papers reporting metabolism of CYA in liver microsomes and intestine, but were limited to metabolite identification; a kinetic analysis of metabolite formation has not been reported. Hence, metabolic parameters cannot be obtained from the literature. In the present model, the *in vivo* hepatic metabolic rate parameters of CYA (Km1) and the intestinal metabolic parameter (Km2) were estimated by manual adjustment until optimal simulations of concentrations of CYA and BDCYA in liver from Li et al. (2013) were obtained. CYA could be extensively metabolised in liver and intestine, with several metabolites formed. The fraction of CYA metabolised into BDCYA in liver and intestine was reported to be 17% and 20%, respectively (Liu et al. 2009; Huang et al. 2015). Based on these results, the formation rate of BDCYA in liver and intestine was described as Km1 and Km2, respectively.

The estimated values for plasma protein binding percentages and renal clearances of CYA and BDCYA are provided in Tables 2 and 3. The mean plasma protein binding percentages of CYA (15%) and BDCYA (72%) calculated from three concentrations were used in the model. The mean renal clearance value for CYA (0.035 ± 0.015 L/h/kg) and BDCYA (0.088 ± 0.044 L/h/kg) was adopted in this model.

Bile excretion of CYA and BDCYA was described with KbC and KbC1, respectively. Their values were estimated by visually fitting the simulated concentrations of CYA and BDCYA in bile to measured data in the radioactivity study (Xu et al. 2012). The final chemical specific parameters for CYA and BDCYA are provided in Tables 2–4.

Exposure paradigm extrapolation

After calibration of the model with the oral gavage dataset, the model was applied to simulate a 60-day feed administration scenario (Qiu 2012). Briefly, 25 healthy castrated crossbred pigs, weighing 30 ± 2.0 kg, were divided into five groups, and fed with medicated feed at the dose of 150 mg/kg for 60 consecutive days. Five pigs were slaughtered at 0.25, 1, 3, 7 and 14 days after the end of exposure, with liver, kidney, muscle and fat samples collected and analysed for CYA and BDCYA using the HPLC method as described above.

Feed intake reduces the gastric emptying rate and decreases the absorption rate of the drug. Therefore, we adjusted Kst, Ka, and Ka1 accordingly by visually fitting to the plasma data from Qiu (2012). Optimal simulations were obtained when Kst, Ka and Ka1 were set to be 0.1,

Table 3. Renal clearance of CYA and BDCYA in pigs.

	Animal number	Concentration in plasma (μg/L)	Concentration in urine (μg/L)	Volume of urine (mL)	Renal clearance (L/h/kg)	Mean ± SD
CYA	1	12.6	306	235	0.478	0.035 ± 0. 015
	2	38.5	194	304	0.128	
	3	20.4	278	323	0.367	
	4	15.6	190	414	0.420	
BDCYA	1	72.9	238	67	0.036	0.0044 ± 0.002
	2	124.2	742	57	0.057	
	3	35.4	163	150	0.115	
	4	140.3	136	898	0.145	

Table 4. Chemical-specific parameters for the development of PBPK model of CYA in pigs.

Parameter	Description	CYA	Sources
BW (kg)	Body weight of the pig	30–50	Li et al. (2013), Qiu (2012)
Absorption			
F	Bioavailability	0.44	Measured from Huang et al. (2015)
Kst (/h)	Emptying rate of stomach	0.2	Buur et al. (2006)
Ka (/h)	Absorption rate constant of CYA	0.0015	Visual fitting based Qiu et al. (2002)
Ka1 (/h)	Absorption rate constant of BDCYA	0.0008	Visual fitting based on Qiu et al. (2002)
PB	Plasma protein binding percentage of CYA	0.153	Measured in Experiment 1
PB1	Plasma protein binding percentage of BDCYA	0.722	Measured in Experiment 1
Partition coefficients			
PLcya	Liver/plasma partition coefficient of CYA	1.0	Visual fitting based on Li et al. (2013)
PKcya	Kidney/plasma partition coefficient of CYA	1.28	Visual fitting based on Li et al. (2013)
PMcya	Muscle/plasma partition coefficient of CYA	4.55	Visual fitting based on Li et al. (2013)
PFcya	Fat/plasma partition coefficient of CYA	1.98	Visual fitting based on Li et al. (2013)
POTcya	Other tissues/plasma partition coefficient of CYA	1.0	Assumed the same as in liver
PLbdcya	Liver/plasma partition coefficient of CYA	0.91	Measured in Experiment 3
PKbdcya	Kidney/plasma partition coefficient of BDCYA	2.87	Measured in Experiment 3
PMbdcya	Muscle/plasma partition coefficient of BDCYA	0.32	Measured in Experiment 3
PFbdcya	Fat/plasma partition coefficient of BDCYA	0.30	Measured in Experiment 3
POTbdcya	Other tissues/plasma partition coefficient of CYA	0.91	Assumed the same as in liver
Metabolism			
Km1 C (/h)	Liver metabolism rate constant	0.01	Visual fitting based on Li et al. (2013)
Km2 C (/h)	Intestinal metabolism rate constant	0.04	Visual fitting based on Li et al. (2013)
FL	Fraction of CYA to be metabolised into BDCYA in liver	0.17	Liu et al. (2009)
FI	Fraction of CYA to be metabolised into BDCYA in intestine	0.2	Xu et al. (2011)
Excretion			
Clcya (L/(h*kg))	Renal clearance of CYA	0.035	Measured in Experiment 2
Clbdcya (L/(h*kg))	Renal clearance of BDCYA L/(h*kg)	0.0044	Measured in Experiment 2
Kef (/h)	Faecal excretion rate constant for CYA	0.4	Visual fitting based on Huang et al. (2015)
Kef1 (/h)	Faecal excretion rate constant for BDCYA	0.2	Visual fitting based on Huang et al. (2015)
Kbc (/h)	Bile elimination rate constant for CYA	0.01	Visual fitting based on Huang et al. (2015)
Kbc1 (/h)	Bile elimination rate constant for BDCYA	0.01	Visual fitting based on Huang et al. (2015)

0.0012 and 0.0006, respectively. In addition, it has been shown that feed administration increased the secretion of bile, the values of KbC and KbC1 were thereby adjusted accordingly by visually fitting to the liver data from Qiu (2012). Optimal simulations were obtained when KbC and KbC1 were set to be 0.015. This model was then used to simulate the tissue concentrations of CYA and BDCYA from Qiu (2012).

Model evaluation

The model was validated using the data from a 14-day consecutive feed administration study described in Experiment 4. All parameters were kept the same as those used for simulating the 60-day feed exposure study. The criterion for a validated model suggested by the World Health Organisation (WHO 2010) was adopted, namely, the predictions that are within a factor of 2 of the

experimental data were considered to be acceptable. When optimal fits could not be achieved across all time points, fitness to later time points were considered more important than earlier time points since the data set was richer at later time points and estimating food safety tissue withdrawal times was the focus of this work.

Sensitivity analysis

A local sensitivity analysis was performed to determine which parameter values were most influential on the $AUC_{0\text{-}7d}$ plasma, liver, kidney, muscle and fat concentrations of CYA and BDCYA. Each parameter was increased by 10% and the corresponding $AUC_{0\text{-}7d}$ concentrations were computed. Normalised sensitivity coefficients (NSCs) were calculated using Equation (7) (Mirfazaelian et al. 2006; Lin et al. 2011):

$$\mathrm{NSC} = \frac{\Delta r}{r} * \frac{\Delta p}{p} \tag{7}$$

where r is the response variable (e.g., AUC plasma concentration for CYA), Δr is the change of the response variable value, p is the value of the parameter of interest (e.g., PC of liver for CYA), and Δp is the change of the parameter value. A parameter was considered influential if NSC reached a minimum absolute value of 0.25 (Leavens et al. 2014).

Uncertainty analysis

Monte Carlo analysis was performed to estimate the prediction variability associated with model parameters. Only those parameters which were shown to be sensitive to the plasma and tissue concentrations were subjected to Monte Carlo analysis. The geometric mean, upper 95th percentile and lower fifth percentile were determined for those parameters. The distributions for these sensitive parameters were taken from the literature or estimated by the model, and are shown in Table 5. The parameters were assumed to be log-normally distributed (Barton et al. 2007; Covington et al. 2007); therefore, the geometric mean of parameter values from all available datasets (Table 5) was used to estimate the central tendency for the parameter. The fifth and 95th percentile values for each parameter were calculated from the standard deviation of the lognormal-transformed estimates for each data set. The fifth and 95th percentile values were used to determine the lower and upper estimate of uncertainty for predicted plasma and tissue concentrations, respectively. Predictions of mean, lower and upper uncertainty of tissue concentrations of CYA and BDCYA in liver, kidney, muscle and fat were compared with reported data (Li et al. 2013; Qiu 2012) and the experimental data generated from this study.

Results

Model calibration

Model predictions of concentrations of CYA and BDCYA in edible tissues at different time points after the last dosing were compared with measured data in pigs dosed orally with 20 mg/kg b.w. CYA for five consecutive days (Li et al. 2013) (Figure 3). Overall, the model accurately simulated the kinetic profiles of CYA and BDCYA in four edible tissues, especially at the later time points (24–120 h) which are important for residue monitoring and the determination of regulatory withdrawal times.

Model simulations showed that parent drug residue concentrations in edible tissues were very low (less than 100 μg/kg) even at the very early withdrawal time of 12 h. BDCYA concentrations in liver and kidney were comparably higher than the parent drug; in contrast the concentrations of parent drug in muscle and fat were slightly higher than BDCYA. Parent drug depleted rapidly in most tissues of pigs with CYA

Table 5. The distribution for the sensitive parameters used in the Monte Carlo analysis.

Parameter	Mean	SD	Upper bound	Lower bound	Data source
CYA					
BW (kg)	50	5.1	51.69	48.31	Li et al. (2013)
Ka (h^{-1})	0.0015	0.0012	0.0023	0.00067	Qiu et al. (2002)
Bio (%)	44.5	3.99	49.52	42.65	Huang et al. (2015)
CLcya (L/h/kg)	0.035	0.015	0.0476	0.0128	Calculated from Experiment 2
Plcya	1.05	0.49	1.5302	0.5698	Estimated based on Li et al. (2013)
Pkcya	1.38	0.83	2.1934	0.5666	
Pmcya	4.55	2.32	6.8236	2.2764	
Pfcya	1.98	1.05	3.009	0.951	
BDCYA					
Ka1(h^{-1})	0.0008	0.00077	0.0015	0.00011	Qiu et al. (2002)
CLbdcya(L/h/kg)	0.0044	0.0025	0.0072	0.0018	Calculated from Experiment 2
Plbdcya	0.91	0.2	1.16	0.66	Calculated from Experiment 3
Pkbdcya	2.27	0.56	3	1.77	Calculated from Experiment 3
Pmbdcya	0.44	0.16	0.6	0.17	Calculated from Experiment 3
Pfbdcya	0.18	0.15	0.18	0.08	Calculated from Experiment 3

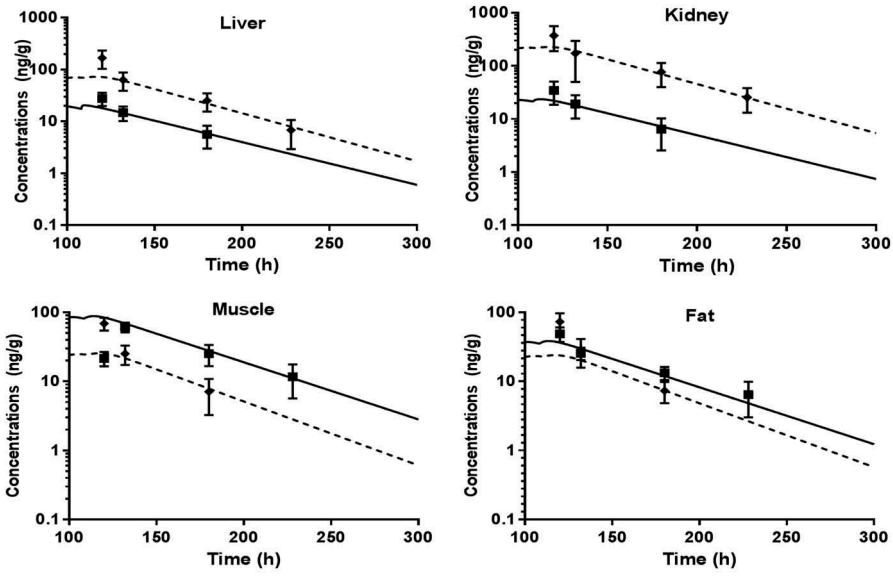

Figure 3. Comparison of model predictions (solid and dotted lines) and measured concentrations of cyadox (solid line, square spot) and bisdesoxycyadox (dotted line, diamond spot) in liver, kidney, muscle and fat of pigs dosed with five consecutive multiple oral gavages of cyadox.

being at 10 μg/kg at 72 h after the last dosing except in muscle. BDCYA depleted comparably slower than the parent drug in liver and kidney, with concentration remaining at 20 μg/kg even 120 h after the last dosing. The highest concentration of BDCYA was observed in kidney. These simulations were consistent with the radiotracer study which showed that BDCYA persisted for the longest time in kidney of pigs (Huang et al. 2015).

Exposure paradigm extrapolation

Following calibration with the oral gavage data sets, the model was extrapolated to simulate a consecutive 60-day exposure study in feed at a dose of 150 mg/kg as reported in Qiu (2012). As shown in Table 6, the model-predicted tissue concentrations of CYA at different withdrawal times were consistent with the experimental data. The concentrations of CYA in muscle and fat were slightly overestimated, but still within two-fold of observed concentrations as deemed acceptable by WHO modelling guidelines. Similarly, the model adequately predicted tissue concentrations of BDCYA at different withdrawal times, except for a slight overestimation (still within a factor of 2) of BDCYA in kidney at 6 h after exposure (Table 6).

Model evaluation

Measured concentrations of CYA and BDCYA in edible tissues of pigs at 6, 24 and 72 h after a consecutive 14-day exposure to CYA in feed were compared with model predictions (Table 7). Overall, the model accurately predicted the tissue concentrations of CYA at different time points (within 1.5–2-fold). The model performed better in predicting BDCYA levels in the four tissues at all time points, except for a slight overestimation at 6 h after exposure in kidney.

Table 6. The predicted and measured concentrations of CYA/BDCYA in edible tissues of pigs dosed with CYA at 150 mg/kg in feed for consecutive 60 days.

		CYA (μg/kg)		BDCYA (μg/kg)	
Tissues	Time	Simulated	Observed[a]	Simulated	Observed[a]
Liver	6	25.4[b]	46.5 ± 9.0	33.3[b]	55.0 ± 8.7
	24	13.5	<20	23.9[b]	20.8 ± 2.5
	72	2.9	<20	6.1	<20
Kidney	6	26.9[b]	27.5 ± 9.0	104.3[b]	59.5 ± 10.7
	24	16.6	<20	75.4[b]	45.1 ± 4.9
	72	3.6	<20	19.3[b]	21.8 ± 2.7
Muscle	6	57.5[b]	38.6 ± 6.3	11.7	<20
	24	35.9	<20	8.5	<20
Fat	6	33.3[b]	22.2 ± 5.7	11.0	<20
	24	20.8	<20	8.0	<20

Notes: [a]Measured levels of CYA and BDCYA in tissues of pigs (Qiu 2012).
[b]Simulated values are within two-fold range of the experimental data.

Parameter sensitivity

Thirty-nine model parameters were subjected to sensitivity analyses for the AUC of CYA and BDCYA in plasma, liver,

Table 7. The predicted and measured concentrations of CYA/BDCYA in edible tissues of pigs dosed with CYA at 200 mg/kg in feed for consecutive 14 days.

		CYA (μg/kg)		BDCYA (μg/kg)	
Tissues	Time	Simulated	Observed[a]	Simulated	Observed[a]
Liver	6	60.2[b]	59.3 ± 5.7	31.3[b]	34.5 ± 5.2
	24	30.3	<20	23.0[b]	24.1 ± 2.5
	72	3.2	<20	5.9	<20
Kidney	6	72.5[b]	66.3 ± 7.2	98.0[b]	66.0 ± 4.4
	24	37.1	<20	72.7[b]	44.2 ± 3.3
	72	3.9	<20	18.7	<20
Muscle	6	43.8[b]	22.5 ± 6.4	11.0	<20
	24	28.6	<20	8.2	<20
Fat	6	40.1[b]	21.9 ± 3.1	10.3	<20
	24	27.5	<20	7.7	<20

Notes: [a]Measured levels of CYA and BDCYA in tissues of pigs. (Please refer to the section of "Experimental study for model development" in the Methods for detailed description of this residue depletion study.)
[b]Simulated values are within two-fold range of the experimental data.

kidney, muscle and fat, resulting in 330 NSCs. The parameters with at least one absolute value of NSC more than or equal to 0.25 were plotted and are presented in Figure 4. All selected AUCs were insensitive to physiological parameters, including blood flow rates and volumes of various tissues. The AUCs of CYA in tissues were moderately negatively sensitive to the liver metabolism rate constant (Km1C) with a NSC value of −0.25, and highly negatively sensitive to body weight (BW), intestinal metabolism rate constant (Km2C) and renal clearance (Clcya) with NSC values of −0.77, −0.77 and −0.62, respectively. The AUC of CYA in plasma was highly negatively sensitive to BW, Km2C and Clcya with NSC values of −0.77, −0.77 and −0.58, respectively. All CYA AUCs were highly positively sensitive to absorption rate constant (Ka) and bioavailability with a NSC value of 1.0.

The AUCs of BDCYA in plasma and tissues were moderately negatively sensitive to liver metabolism rate constant Clbdcya with a NSC value of −0.26 and highly negatively sensitive to intestinal transit rate constant (Kef1) and bile elimination rate constant of BDCYA (Kbc1) with NSC values being −0.88 and −0.64, respectively. All AUCs of BDCYA were highly positively sensitive to absorption rate constant of BDCYA (Ka) and bioavailability of CYA with NSC values of 0.97 and 1.0, respectively. Moreover, the AUCs of CYA and BDCYA in four edible tissues were highly positively sensitive to the corresponding partition coefficient (PC) with NSC values near to 1.0.

Monte Carlo analysis

All the sensitive parameters identified above were subjected to Monte Carlo analyses for each tissue, resulting in 76 simulation results. The representative Monte Carlo simulations based on the most sensitive parameters (Ka and Ka1 for CYA and BDCYA, respectively) were compared to measured concentrations in tissues of individual pigs after 5-day oral exposure as presented in Figure 5. The measured individual concentrations generally fell in the range of predicted concentrations, except for a slight underestimation of CYA concentrations in liver and kidney, as well as BDCYA concentrations in muscle and fat, at the early time point of 12 h. Notably, the measured concentrations of both CYA and BDCYA at terminal elimination time points, most relevant to residue monitoring and withdrawal time determination, were well covered by the Monte Carlo simulations.

Discussion

A PBPK model was developed for CYA and its marker residue BDCYA after oral administration in pigs, and then scaled to longer term administration in feed. This is the first PBPK model that simulates the distribution and depletion of both the parent drug and its marker metabolite in edible tissues of a food animal species. The model

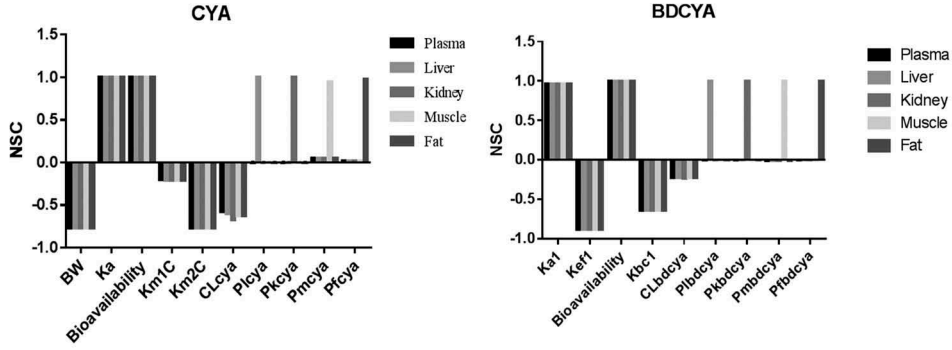

Figure 4. Normalised sensitivity coefficients (NSCs) of several sensitive model parameters using AUCs for CYA and BDCYA concentrations in plasma, liver, kidney, muscle and fat as the dose metrics. The simulations were based on five consecutive oral exposures at 20 mg/kg b.w.

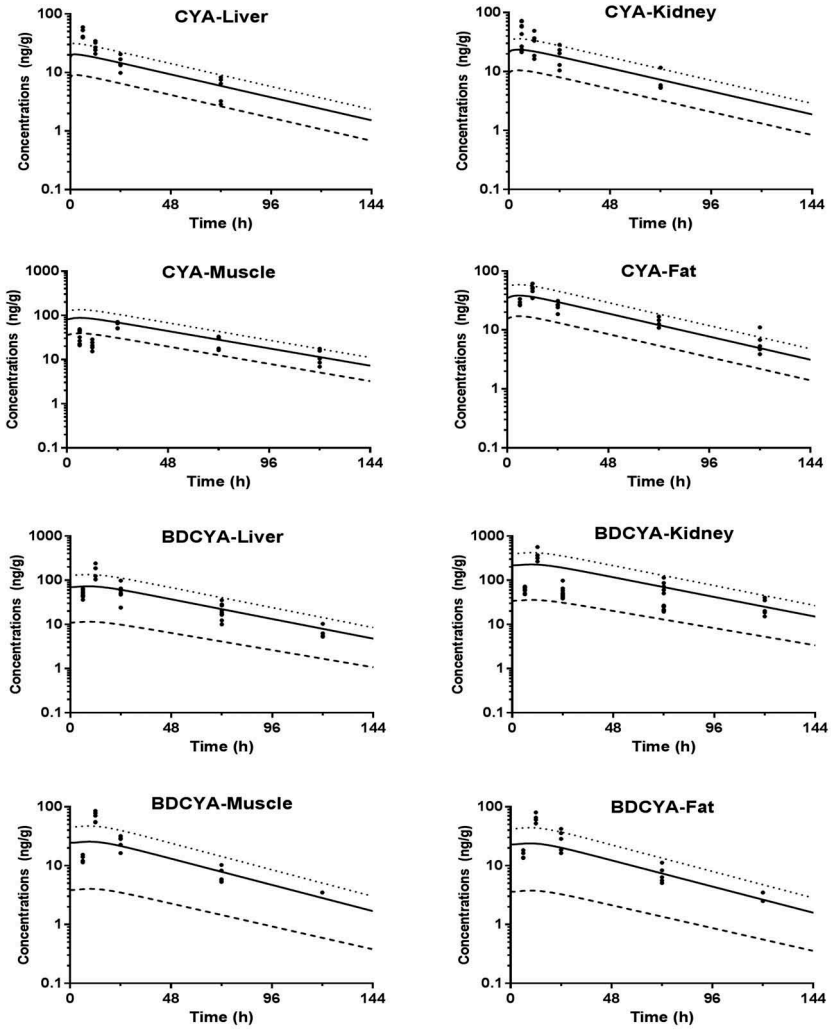

Figure 5. Monte Carlo simulations for CYA and BDCYA concentrations in edible tissues after consecutive 5-day oral exposure (20 mg/kg b.w.). Solid symbols represent observed values from reported data (Li et al. 2013) and experimental data in this study for individual pigs. Solid lines represent the mean simulated concentrations; thick dashed lines are the lower simulated concentrations with 5% percentage; shallow dotted lines are the upper simulated concentrations with 95% percentage.

accurately predicted CYA and BDCYA distribution and depletion in food-safety-relevant and residue-monitored edible tissues. The model predicted that relatively low residue quantities of CYA (<100 μg/kg) would occur in pig tissues after oral dosage of 20 mg/kg even at an early withdrawal time of 12 h. BDCYA was the main residue in pig liver and kidney having higher concentrations and persisting longer than CYA.

Compared with traditional or population-based pharmacokinetic models (Li et al. 2015), it is apparent that PBPK models have great advantages in predicting drug tissue residues and withdrawal times. PBPK models provide more comprehensive simulation of drug disposition characteristics because PBPK model compartments are physiologically based. Thus, PBPK models could be used to predict the concentration of parent drug and/or a key metabolite in a specific target tissue of interest at any time points after a complex exposure paradigm. From food safety perspective, it is understandable that liver, kidney, muscle, and fat should be included as individual compartments as these organs are edible tissues. In addition, it should be noted that the biodistribution of a drug is dependent upon its disposition in all tissues with plasma as the conduit distributing drug throughout the body. This is why the blood and other organs should be included as separated compartments. The strength of a PBPK model is that data which describes these processes can be directly incorporated into the model to reduce uncertainty in the tissue residue predictions. It also allows simulations on altered organ function (e.g., due to disease states or other physiological variables) to be used to assess their

impact on tissue residue withdrawal. Other empirical methods confound biodistribution and elimination processes with random error in only analysing tissue depletion.

A PBPK model was recently published for CYA's other metabolite, QCA, in rats and pigs (Yang et al. 2015). In contrast to the present work, it was limited to the description of the kinetics of the metabolite, but not the parent compound. Furthermore, QCA was considered as a key metabolite of CYA for residue control in that work. In contrast, BDCYA was selected as a marker residue in the present study, which appears appropriate based on a recent radiotracer study (Huang et al. 2015) that showed BDCYA was better associated with residue monitoring and determination of CYA withdrawal times. Moreover, in the previous model, liver was considered to be the sole site of biotransformation (Yang et al. 2015). Since it had been demonstrated that CYA could be metabolised by intestinal microsomes and microbial flora, and radiotracer was observed both in faeces and bile as well as urine (Huang et al. 2015), the present model incorporated these dynamic processes to more comprehensively describe the depletion of CYA and BDCYA in pigs.

A realistic feed exposure scenario was developed based on the oral gavage model to simulate the depletion of CYA and BDCYA in edible tissues after drug exposure in feed, which is more closely related to actual field usage. The present model provides a realistic simulation of CYA and BDCYA concentrations in plasma and edible tissues of pigs, which is informative for the design of dosage regimens and food safety control points. Use of such models to predict residue depletion and withdrawal time determination should be more widely adopted. This is especially true for drugs whose marker residues are metabolites that often assume a simple fixed ratio to parent drug concentration, a practice shown to be in error based upon the PBPK simulations as presented here. There is no reason to believe that cyadox is unique in this regard.

Liver and intestine were found to be the main sites of biotransformation based on the *in vitro* metabolism studies (Liu et al. 2009; Xu et al. 2011). Although more than ten metabolites were produced when CYA was fed to pigs, some minor intermediate metabolites were described. The interaction of these metabolites with organs were considered minor pathways, and a "one-step" major metabolism pathway for marker residue was used as described by Corley et al. (2005). Normally a Michaelis-Menten equation is used to describe the metabolism of exogenous compounds in the body. However, the amount of BDCYA linearly increased with CYA incubation with liver microsomes over time, showing first-order kinetics (Zhang et al. 2015). Therefore, several first-order rate constants Km1C and Km2C, instead of V_{max} and K_m, were used to describe the average rate of CYA metabolite formation, and then the fraction of BDCYA to total metabolites was assigned to describe BDCYA formation in liver and intestine based on the liver microsomal metabolism data in Liu et al. (2009) and intestinal microbial flora data in Xu et al. (2011). This approach is consistent with the use of first-order rate constants in several earlier PBPK models to describe the drug biotransformation (Buur et al. 2005; Yang, Sun, et al. 2014).

As seen from the sensitivity analysis, many parameters were influential on the predictions of tissue concentrations. In particular, absorption constants, including Ka, Ka1 and bioavailability, were the most important factors. Body weight was also influential on the prediction of the tissue concentration. Body weight was fixed during the calibration of the model because of short study period (5 days). Since CYA was a feed additive used in feed for long time, a weight gain equation based on the results of growth experiment (Wang et al. 2005) was applied in the feed exposure model to reflect the influence of increasing body weight on CYA and BDCYA concentrations.

Metabolic rate constants, as expected, were also influential in determining the concentrations of CYA in plasma and tissues. N-oxide reduction is the predominant metabolic pathway of CYA in pigs (Liu et al. 2009). Xanthine oxidoreductase (XOR) and aldehyde oxidase (AO) are the key enzymes to catalyse the N-oxide reduction of quinoxaline 1,4-di-N-oxides (Liu et al. 2009; Zheng et al. 2011; Cheng et al. 2013; Mu et al. 2014). Hence, the amount and activity of xanthine oxidoreductase and aldehyde oxidase in liver and intestine determine the rate of CYA metabolism. Up to now, there has been no data on the specific amount and activity of these enzymes in pigs. It has been demonstrated that XOR activity is widely detected in various mammalian tissues including as rats and human, with the highest levels being found in liver and intestine (Krenitisky et al. 1974; Parks & Granger 1986). XOR mRNA levels were also found to be the highest in liver and intestine of mice and humans (Sarnesto et al. 1996; Saksela et al. 1998). Based on these findings, the metabolic rate constants of CYA in liver and intestine were set to be the same in this model.

Monte Carlo simulations were conducted to estimate the prediction variability caused by differences between individuals in the present model. The broadest ranges of values for the sensitive parameter (Ka) were used to reflect the maximum variation of the tissue concentration. The wider distributions could result in widening of the overall spread of Monte Carlo outputs and overestimation of population variance. In its application to the present model, this limitation would produce a more

conservative estimate of withdrawal time (Buur et al. 2006). The results of Monte Carlo simulations revealed an excellent coverage between the estimated distributions and observed data, suggesting the present PBPK model has the potential to predict the population kinetics of CYA and BDCAY residues in pigs. Nevertheless, further studies are needed to update the model and narrow the prediction variability of the model as data on the true distributions of the sensitive parameters are generated. More sophisticated stochastic approaches to estimate these distributions based on physiological data could then be applied.

In conclusion, the first PBPK model that simultaneously simulates CYA and BDCYA concentrations in edible tissues of pigs following oral dosing and prolonged feed administration was developed based on reported data and several additional experiments in this study. A satisfactory simulation of CYA and BDCYA concentrations in edible tissues was obtained. Prediction variability of the model was estimated based on Monte Carlo simulations, showing a good coverage of experimental data. This model provides a foundation for creating PBPK models for other veterinary drugs to simultaneously simulate the kinetics of both parent compounds and metabolites to better predict tissue residues under varying physiological conditions, disease states, and routes of drug administration encountered in the field.

Disclosure statement

No potential conflict of interest was reported by the authors.

Funding

The authors are thankful for the financial support from National Risk Assessment Program of Quality and Safety of Livestock and Poultry Products (GJFP2014007), Recommend International Advanced Agricultural Science and Technology Plan (No. 2011-G4), and The Kansas Bioscience Authority funds to the Institute of Computational Comparative Medicine (ICCM) at Kansas State University.

References

[AVMA] American Veterinary Medical Association. 2001. Panel on Euthanasia 2000 Report of the AVMA panel on euthanasia. J Am Vet Med A. 218:669–696.

Badham HJ, Winn LM. 2010. In utero exposure to benzene disrupts fetal hematopoietic progenitor cell growth via reactive oxygen species. Toxicol Sci. 113:207–215.

Barton HA, Chiu WA, Setzer RW, Andersen ME, Bailer AJ, Bois FY, Dewoskin RS, Hays S, Johanson G, Jones N. 2007. Characterising uncertainty and variability in physiologically based pharmacokinetic models: state of the science and needs for research and implementation. Toxicol Sci. 99:395–402.

Baynes RE, Riviere JE. 2014. Strategies for reducing drug and chemical residues in food animals: international approaches to residue avoidance, management, and testing. 1st ed. Hoboken (NJ): Wiley & Sons.

Buur JL, Baynes R, Smith G, Riviere JE. 2006. Use of probabilistic modeling within a physiologically based pharmacokinetic model to predict sulfamethazine residue withdrawal times in edible tissues in swine. Antimicrob Agents Chemother. 50:2344–2351.

Buur JL, Baynes RE, Craigmill AL, Riviere JE. 2005. Development of a physiologic-based pharmacokinetic model for estimating sulfamethazine concentrations in swine and application to prediction of violative residues in edible tissues. Am J Vet Res. 66:1686–1693.

Buur JL, Baynes RE, Riviere JE. 2008. Estimating meat withdrawal times in pigs exposed to melamine contaminated feed using a physiologically based pharmacokinetic model. Regul Toxicol Pharmacol. 51:324–331.

Cheng XG, Ju WZ, Dai GL, Ma S, Tan HS. 2013. Plasma protein binding rate of procyanidin B2, epicatechin by equilibrium dialysis method in human plasma. Chinese Pharmacol Bullet. 29:1465–1467.

Chiesa OA, Von Bredow J, Nochetto C, Smith M, Heller D, Moulton K, Thomas MH. 2006. Use of tissue-fluid correlations to estimate gentamicin residues in kidney tissue of Holstein steers. J Vet Pharmacol Ther. 29:99–106.

Chiesa OA, Von Bredow J, Smith M, Heller D, Condon R, Thomas MH. 2006. Bovine kidney tissue/biological fluid correlation for penicillin. J Vet Pharmacol Ther. 29:299–306.

Corley RA, Bartels MJ, Carney EW, Weitz KK, Soelberg JJ, Gies RA, Thrall KD. 2005 Development of a physiologically based pharmacokinetic model for ethylene glycol and its metabolite, glycolic Acid, in rats and humans. Toxicol Sci. 85:476–490.

Cortright KA, Wetzlich SE, Craigmill AL. 2009. A PBPK model for midazolam in four avian species. J Vet Pharmacol Ther. 32:552–565.

Covington TR, Gentry PR, Van Landingham CB, Andersen ME, Kester JE, Clewell HJ. 2007. The use of Markov chain Monte Carlo uncertainty analysis to support a public health goal for perchloroethylene. Regul Toxicol Pharmacol. 47:1–18.

Craigmill AL. 2003. A physiologically based pharmacokinetic model for oxytetracycline residues in sheep. J Vet Pharmacol Ther. 26:55–63.

Ding MX, Wang YL, Zhu HL, Yuan ZH. 2006. Effects of cyadox and olaquindox on intestinal mucosal immunity and on fecal shedding of Escherichia coli in piglets. J Anim Sci. 84:2367–2373.

Ding MX, Yuan ZH, Wang YL, Zhu HL, Fan SX. 2006. Olaquindox and cyadox stimulate growth and decrease intestinal mucosal immunity of piglets orally inoculated with Escherichia coli. J Anim Physiol Anim Nutr. 90:238–243.

Hao H, Guo W, Iqbal Z, Cheng G, Wang X, Dai M, Huang L, Wang Y, Peng D, Liu Z, et al. 2013. Impact of cyadox on human colonic microflora in chemostat models. Regul Toxicol Pharmacol. 67:335–343.

He QH, Fang GJ, Wang YL, Wei ZC, Wang DJ, Zhou SQ, Sx F, Yuan ZH. 2006. Experimental evaluation of cyadox phototoxicity to Balb/c mouse skin. Photodermatol Photo. 22:100–104.

Huang C, Lei H, Zhao X, Tang H, Wang Y. 2013. Metabolic influence of acute cyadox exposure on Kunming mice. J Proteome Res. 12:537–545.

Huang LL, Xu N, Sechenchogt H, Pan YH, Chen DM, Tao YF, Liu ZL, Yuan ZH. 2015. Metabolic disposition and

elimination of cyadox in pigs, chickens, carp and rats. J Agr Food Chem. 63:5557–5569.

Huang X-J, Zhang -H-H, Wang X, Huang -L-L, Zhang L-Y, Yan C-X, Liu Y, Yuan Z-H. 2010. ROS mediated cytotoxicity of porcine adrenocortical cells induced by QdNOs derivatives in vitro. Chem Biol Interact. 185:227–234.

Krenitisky TA, Tuttle JV, Cattau EL, Wang P. 1974. A comparison of the distribution and electron acceptor specificities of xanthine oxidase and aldehyde oxidase. Comp Biochem Physiol. 49B:687–703.

Leavens TL, Tell LA, Clothier KA, Griffith RW, Baynes RE, Riviere JE. 2012. Development of a physiologically based pharmacokinetic model to predict tulathromycin distribution in goats. J Vet Pharmacol Ther. 35:121–131.

Leavens TL, Tell LA, Kissell LW, Smith GW, Smith DJ, Wagner SA, Shelver WL, Wu H, Baynes RE, Riviere JE. 2014. Development of a physiologically based pharmacokinetic model for flunixin in cattle (Bos taurus). Food Addit Contam A. 31:1506–1521.

Li M, Gehring R, Lin Z, Riviere J. 2015. A framework for meta-analysis of veterinary drug pharmacokinetic data using mixed effect modeling. J Pharm Sci. 104:1230–1239.

Li YF, Zhao N, Zeng ZL, Gu XY, Fang BH, Yang F, Zhang BX, Ding HZ. 2013. Tissue deposition and residue depletion of cyadox and its three major metabolites in pigs after oral administration. J Agric Food Chem. 61:9510–9515.

Lin Z, Fisher JW, Ross MK, Filipov NM. 2011. A physiologically based pharmacokinetic model for atrazine and its main metabolites in the adult male C57BL/6 mouse. Toxicol Appl Pharmacol. 251:16–31.

Lin Z, Fisher JW, Wang R, Ross MK, Filipov NM. 2013. Estimation of placental and lactational transfer and tissue distribution of atrazine and its main metabolites in rodent dams, fetuses, and neonates with physiologically based pharmacokinetic modeling. Toxicol Appl Pharmacol. 273:140–158.

Lin Z, Li M, Gehring R, Riviere JE. 2015. Development and application of a multiroute physiologically based pharmacokinetic model for oxytetracycline in dogs and humans. J Pharm Sci. 104:233–243.

Liu ZY, Huang LL, Dai MH, Chen DM, Tao YF, Wang YL, Yuan ZH. 2009. Metabolism of cyadox in rat, chickens and pig liver microsomes and identification of metabolites by accurate mass measurements using electrospray ionization hybrid ion trap/time-of-flight mass spectrometry. Rapid Commun. Mass Spectrom. 23:2026–2034.

Liu Y, Huang LL, Wang YL, Yang B, Ishan A, Fang K, Peng DP, Liu ZL, Dai MH, Yuan ZH. 2010. Tissue depletion and concentration correlations between edible tissues and biological fluids of 3-amino-2-oxazolidinone in pigs fed with a furazolidone medicated feed. J Agric Food Chem. 58:6774–6779.

Mercer HD, Baggot JD, Sams RA. 1977. Application of pharmacokinetic methods to the drug residue profile. J Toxicol Environ Health. 2:787–801.

Mirfazaelian A, Kim KB, Anand SS, Kim HJ, Tornero-Velez R, Bruckner JV, Fisher JW. 2006. Development of a physiologically based pharmacokinetic model for deltamethrin in the adult male Sprague-Dawley rat. Toxicol Sci. 93:432–442.

Mu P, Zheng M, Xu M, Zheng Y, Tang X, Wang Y, Wu K, Chen Q, Wang L, Deng Y. 2014. N-oxide reduction of quinoxaline-1,4-dioxides catalyzed by porcine aldehyde oxidase SsAOX1. Drug Metab Dispos. 42:511–519.

Parks DA, Granger DN. 1986. Xanthine oxidase: biochemistry, distribution and physiology. Acta Physiol Scand. 548:87–99.

Qiu YM. 2012. Residue depletion of cyadox in pigs, chickens and carp [master dissertation]. Wuhan: Huazhong Agricultural University.

Qiu YS, Fan SX, Liu DC, Huang LL, Yin JY. 2002. Determination of Cyadox and Bisdesoxycyadox in plasma and edible tissues using high-performance liquid chromatography. Chinese J Vet Sci. 23:363–365.

Riviere JE. 2011. Comparative Pharmacokinetics: Principles, Techniques, and Applications. 2nd ed. Ames, IA: Wiley-Blackwell.

Saksela M, Lapatto R, Raivio KO. 1998. Xanthine oxidoreductase gene expression and enzyme activity in developing human tissues. Biol Neonate. 74:274–280.

Sarnesto A, Linder N, Raivio KO. 1996. Organ distribution and molecular forms of human xanthine dehydrogenase, xanthine oxidase protein. Lab Invest. 74:48–56.

Tranquilli WJ, Parks CM, Thurmon JC, Benson GJ, Koritz GD, Manohar M, Theodorakis MC. 1982. Organ blood flow and distribution of cardiac output in nonanesthetized swine. Am J Vet Res. 43:895–897.

Upton RN. 2008. Organ weights and blood flows of sheep and pig for physiological pharmacokinetic modelling. Pharmacol Toxicol Methods. 58:198–205.

Wang X, Fang G-J, Wang Y-L, Ihsan A, Huang -L-L, Zhou W, Liu Z-L, Yuan Z-H. 2011. Two generation reproduction and teratogenicity studies of feeding cyadox in Wistar rats. Food Chem Toxicol. 49:1068–1079.

Wang X, He Q-H, Wang Y-L, Ihsan A, Huang -L-L, Zhou W, Su S-J, Liu Z-L, Yuan Z-H. 2011. A chronic toxicity study of cyadox in Wistar rats. Regul Toxicol Pharm. 59:324–333.

Wang YL, Yuan ZH, Zhu HL, Ding MX, Fan SX. 2005. Effect of cyadox on growth and nutrient digestibility in weanling pigs. S Afr J Anim Sci. 35:117–125.

[WHO] World Health Organisation. 2010. Characterization and application of physiologically based pharmaco-kinetic models in risk assessment. Geneva: World Health Organization; p. 21–37.

Wu HX, Li LX, Shen JZ, Wang Y, Liu KL, Zhang SX. 2012. In vitro metabolism of cyadox in rat, chicken and swine using ultra-performance liquid chromatography quadrupole time-of-flight mass spectrometry. J Pharmaceut Biomed Anal. 67-68:175–185.

Xu N, Huang LL, Liu ZY, Pan YH, Wang X, Tao YF, Chen DM, Wang YL, Peng DP, Yuan ZH. 2011. Metabolism of cyadox by the intestinal mucosa microsomes and gut flora of swine, and identification of metabolites by high-performance liquid chromatography combined with ion trap/time-of-flight mass spectrometry. Rapid Commun Mass Spectrom. 25:2333–2344.

Yang B, Huang LL, Fang K, Wang YL, Peng DP, Liu ZL, Yuan ZH. 2014. A physiologically based pharmacokinetic model for the prediction of the depletion of methyl-3-quinoxaline-2-carboxylic acid, the marker residue of olaquindox, in the edible tissues of pigs. J Vet Pharmacol Ther. 37:66–82.

Yang B, Huang LL, Wang YL, Liu Y, Tao YF, Chen DM, Liu ZL, Fang K, Chen YP, Yuan ZH. 2010. Residue depletion and tissue-plasma correlation of methyl-3-quinoxaline-2-carboxylic acid after dietary administration of olaquindox in pigs. J Agric Food Chem. 58:937–942.

Yang F, Sun N, Liu YM, Zeng ZL. 2014. Estimating danofloxacin withdrawal time in broiler chickens based on

physiologically based pharmacokinetics modeling. J Vet Pharmacol Ther. 37:579–588. [Epub ahead of print].

Yang X, Zhou Y-F, Yu Y, Zhao D-H, Shi W, Fang B-H, Liu Y-H. 2015. A physiologically based pharmacokinetic model for quinoxaline-2-carboxylic acid in rats, extrapolation to pigs. J Vet Pharmacol Ther. 38:55–64.

Zhang HH, Wang X, Huang LL, Pan YH, Li J, Chen DM, Cheng GY, Hao HH, Tao YF, Liu ZL, Yuan ZH. 2015. Deoxidation rates play a critical role in DNA damage mediated by important synthetic drugs, quinoxaline 1,4-dioxides. Chem Res Toxicol. 28:470–481.

Zhang YL, Huang LL, Chen DM, Fan SX, Wang YL, Tao YF, Yuan ZH. 2005. Development of HPLC methods for determination of cyadox and its main metabolites in goat tissues. Analyt Sci. 21:1495–1499.

Zhao N, Wang L, Lu -X-X, Jia H-Q, Fang B-H, Zeng Z-L, Ding H-Z. 2013. Pharmacokinetics of cyadox and its major metabolites in swine after intravenous and oral administration. J Integ Agric. 12:495–501.

Zheng M, Jiang J, Wang J, Tang X, Ouyang M, Deng Y. 2011. The mechanism of enzymatic and non-enzymatic N-oxide reductive metabolism of cyadox in pig liver. Xenobiotica. 41:964–971.